VU VRIJE UNIVERSITEIT AMSTERDAM

VU Research Portal

Finite element modeling of aponeurotomy: altered intramuscular myofascial force transmission yields complex sarcomere length distributions determining acute effects

Yucesoy, C.A.; Koopman, B.H.; Grootenboer, H.J.; Huijing, P.A.J.B.M.

published in
Biomechanics and Modeling in Mechanobiology
2007

DOI (link to publisher)
10.1007/s10237-006-0051-0

document version
Publisher's PDF, also known as Version of record

Link to publication in VU Research Portal

citation for published version (APA)
Yucesoy, C. A., Koopman, B. H., Grootenboer, H. J., & Huijing, P. A. J. B. M. (2007). Finite element modeling of aponeurotomy: altered intramuscular myofascial force transmission yields complex sarcomere length distributions determining acute effects. *Biomechanics and Modeling in Mechanobiology*, *6*, 227-243. https://doi.org/10.1007/s10237-006-0051-0

General rights
Copyright and moral rights for the publications made accessible in the public portal are retained by the authors and/or other copyright owners and it is a condition of accessing publications that users recognise and abide by the legal requirements associated with these rights.

- Users may download and print one copy of any publication from the public portal for the purpose of private study or research.
- You may not further distribute the material or use it for any profit-making activity or commercial gain
- You may freely distribute the URL identifying the publication in the public portal

Take down policy
If you believe that this document breaches copyright please contact us providing details, and we will remove access to the work immediately and investigate your claim.

E-mail address:
vuresearchportal.ub@vu.nl

Download date: 26. Mar. 2026

Biomechan Model Mechanobiol (2007) 6:227–243
DOI 10.1007/s10237-006-0051-0

ORIGINAL PAPER

Finite element modeling of aponeurotomy: altered intramuscular myofascial force transmission yields complex sarcomere length distributions determining acute effects

Can A. Yucesoy · Bart H. F. J. M. Koopman · Henk J. Grootenboer · Peter A. Huijing

Received: 16 September 2005 / Accepted: 13 April 2006 / Published online: 9 August 2006
© Springer-Verlag 2006

Abstract Finite element modeling of aponeurotomized rat extensor digitorium longus muscle was performed to investigate the acute effects of proximal aponeurotomy. The specific goal was to assess the changes in lengths of sarcomeres within aponeurotomized muscle and to explain how the intervention leads to alterations in muscle length–force characteristics. Major changes in muscle length–active force characteristics were shown for the aponeurotomized muscle modeled with (1) only a discontinuity in the proximal aponeurosis and (2) with additional discontinuities of the muscles' extracellular matrix (i.e., when both myotendinous and myofascial force transmission mechanisms are interfered with). After muscle lengthening, two cut ends of the aponeurosis were separated by a gap. After intervention (1), only active slack length increased (by approximately 0.9 mm) and limited reductions in muscle active force were found (e.g., muscle optimum force decreased by only 1%) After intervention (2) active slack increased further (by 1.2 mm) and optimum length as well (by 2.0 mm) shifted and the range between these lengths increased. In addition, muscle active force was reduced substantially (e.g., muscle optimum force decreased by 21%). The modeled tearing of the intramuscular connective tissue divides the muscle into a proximal and a distal population of muscle fibers. The altered force transmission was shown to lead to major sarcomere length distributions [not encountered in the intact muscle and after intervention (1)], with contrasting effects for the two muscle fiber populations: (a) Within the distal population (i.e. fibers with no myotendinous connection to the muscles' origin), sarcomeres were much shorter than within the proximal population (fibers with intact myotendinous junction at both ends). (b) Within the distal population, from proximal ends of muscle fibers to distal ends, the serial distribution of sarcomere lengths ranged from the lowest length to high lengths. In contrast within the proximal population, the direction of the distribution was reversed. Such differences in distribution of sarcomere lengths between the proximal and distal fiber populations explain the shifts in muscle active slack and optimal lengths. Muscle force reduction after intervention (2) is explained primarily by the short sarcomeres within the distal population. However, fiber stress distributions showed contribution of the majority of the sarcomeres to muscle force: myofascial force transmission prevents the sarcomeres from shortening to nonphysiological lengths. It is concluded that interfering with the intramuscular myofascial force transmission due to rupturing of the intramuscular connective tissue leads to a complex distribution of sarcomere lengths within the aponeurotomized muscle and this determines the acute effects of the intervention on muscle length–force characteristics rather than the intervention with the myotendinous force transmission after which the intervention was named. These results

C. A. Yucesoy (✉) · P. A. Huijing
Instituut voor Fundamentele en Klinische Bewegingswetenschappen, Faculteit Bewegingswetenschappen, Vrije Universiteit, Amsterdam, The Netherlands
e-mail: can.yucesoy@boun.edu.tr

C. A. Yucesoy · B. H. F. J. M. Koopman · H. J. Grootenboer · P. A. Huijing
Integrated Biomedical Engineering for Restoration of Human Function, Faculteit Constructieve Technische Wetenschappen, Universiteit Twente, Enschede, The Netherlands

C. A. Yucesoy
Biomedical Engineering Institute, Boğaziçi University, 34342 Bebek – Istanbul, Turkey

suggest that during surgery, but also postoperatively, major attention should be focused on the length and activity of aponeurotomized muscle, as changes in connective tissue tear depth will affect the acute effects of the intervention.

Keywords Aponeurotomy · Myofascial force transmission · Muscle length–force characteristics · Sarcomere length distributions · Finite element method · Rat extensor digitorium longus (EDL) muscle

1 Introduction

Aponeurotomy is a surgical technique (e.g. Baumann and Koch 1989) executed to correct functional problems due to contractures occurring in spastic paresis. A transverse cut made through the intramuscular aponeurosis yields progressive rupturing of the connective tissue below the location of the intervention after isometric lengthening (Jaspers et al. 1999). Although clinical success in lengthening of muscle and restoring function after the intervention was reported (e.g. Nather et al. 1984; Reimers 1990; Nene et al. 1993), the recurrence rate is fairly high (Ejeskar 1982; Olney et al. 1988). Also the mechanism for the effects of aponeurotomy is not clearly understood.

Skeletal muscle is commonly considered to be comprised of muscle fibers that are independent of each other. This means that force transmission via the connections between adjacent myofibrils to transsarcolemmal proteins connecting peripheral myofibrils to the extracellular matrix (ECM) along the full length of the muscle fiber (for a review see Berthier and Blaineau 1997) is not accounted for (e.g. Hawkins and Bey 1997). Owing to this, in studies on effects and possible correction of deformities in spastic paresis, single samples of sarcomere length have been considered as being representative of the lengths of sarcomeres within muscle fibers or even of the entire muscle (e.g. Lieber and Friden 1997).

However, the continuous system of connective tissues has been shown experimentally to transmit force from single isolated muscle fibers (Ramsey and Street 1940), within isolated fascicles (Street and Ramsey 1965; Street 1983) within a dissected muscle in situ (e.g. Trotter and Purslow 1992; Hijikata et al. 1993; Trotter et al. 1995; Huijing et al. 1998; Huijing 1999a,b), and also using finite element modeling (Yucesoy et al. 2002). Such force transmission is referred to as intramuscular myofascial force transmission (Huijing 1999a,b). This indicates that mechanical interaction occurs not only between sarcomeres arranged in series within muscle fibers, but also between sarcomeres located in neighboring muscle fibers.

Recent experiments on rat muscles improved the understanding of the acute physiological effects of aponeurotomy (Jaspers et al. 1999, 2002; Brunner et al. 2000) and in the long term (Brunner et al. 2000). These studies showed altered muscle length–force characteristics as well as substantial changes in muscle fiber lengths. Taking into account intramuscular myofascial force transmission, such results have lead to postulation of a sizable inhomogeneity in the lengths of sarcomeres within muscle fibers as an acute effect of aponeurotomy.

Modeling skeletal muscle mechanics using finite element method allows considering muscle tissue as a continuum and material and geometric nonlinearities can be accounted for. This approach has been used successfully (e.g. Gielen 1998; van der Linden 1998; Johansson et al. 2000; Oomens et al. 2003). Recently, we developed a model in order to study the effects of myofascial force transmission explicitly (Yucesoy et al. 2002). In this model, instead of using elements in which both active and passive properties of muscle tissue are lumped, a two-domain approach is employed: the intracellular and the extracellular matrix domains of skeletal muscle are represented by two separate but elastically linked meshes. In the present study, acute effects of aponeurotomy are studied using this model.

In contrast to experiments, modeling allows two types of effects of aponeurotomy to be distinguished: (1) The effects of a discontinuity within the sectioned aponeurosis (interfering exclusively with the myotendinous force transmission pathway of distal muscle fibers) and (2) discontinuity within the intramuscular extracellular matrix (partially interfering with intramuscular myofascial force transmission pathways).

Our first goal was to assess the effects of the interventions on distribution of lengths of sarcomeres within the muscle fibers and to explain how the interventions lead to changes in muscle length–force characteristics.

Our second goal was to determine which of these force transmission mechanisms dominate the acute effects of the intervention.

2 Methods

2.1 Description of the "linked fiber–matrix mesh model"

In the linked fiber–matrix mesh model (lfmm model), skeletal muscle is considered explicitly as two separate domains: (1) the intracellular domain and (2) ECM domain. The transsarcolemmal attachments are considered as elastic links between the two domains (Yucesoy et al. 2002).

Two self-programmed elements were developed and were introduced as user-defined elements into the finite element program ANSYS 9.0. One of these elements represents the ECM, which includes the basal lamina and connective tissue components such as endomysium and perimysium (*extracellular matrix element*). A second element models the muscle fibers (*myofiber element*). Within the biological context, the combined *muscle element* represents a segment of a bundle of muscle fibers with identical material properties, its connective tissues and the links between them. This is realized as a linked system of ECM and myofiber elements. A schematic 2D representation of an arrangement of these muscle elements is shown in Fig. 2a.

In the lfmm model, the ECM domain is represented by a mesh of ECM elements (*matrix mesh*). In the same space, a separate mesh of myofiber elements is built to represent the intracellular domain (*fiber mesh*). The two meshes are rigidly connected to single layers of elements modeling proximal and distal aponeuroses at the myotendinous connection sites and are linked elastically at the intermediate nodes.

Both ECM and myofiber elements have eight nodes, linear interpolation functions and a large deformation analysis formulation. A 3D local coordinate system representing the fiber, cross-fiber (normal to the fiber direction), and thickness directions is used. The stress formulation, $\underline{S}$ based on Second Piola–Kirchoff definition constitutes the derivative of the strain energy density function, W with respect to the Green–Lagrange strain tensor, $\mathrm{d}\underline{L}^G$

$$\underline{S} = \frac{\mathrm{d}W}{\mathrm{d}\underline{L}^G} \tag{1}$$

2.1.1 Extracellular matrix element

The strain energy density function mechanically characterizing the ECM includes two parts:

$$W = W_1 + W_2. \tag{2}$$

The first part represents the nonlinear and anisotropic material properties (Huyghe et al. 1991):

$$W_1 = W_{ij}(\varepsilon_{ij}) \tag{3}$$

where

$$\begin{aligned} &W_{ij}(\varepsilon_{ij}) = k(e^{a_{ij}\varepsilon_{ij}} - a_{ij} - \varepsilon_{ij}) \text{ for } \varepsilon_{ij} > 0 \text{ or} \\ &W_{ij}(\varepsilon_{ij}) = -W_{ij}\big(|\varepsilon_{ij}|\big) \text{ for } \varepsilon_{ij} < 0 \text{ and } i \neq j \end{aligned} \tag{4}$$

ε_{ij} are the Green–Lagrange strains in the local coordinates. The indices $i = 1,\ldots,3$ and $j = 1,\ldots,3$ represent the local cross-fiber, fiber and thickness directions, respectively. a_{ij} and k are constants (Table 1). The resulting stress–strain curves are shown in Fig. 1a.

The second part includes a penalty function to account for the constancy of muscle volume.

$$W_2 = S_\mathrm{s}(I_3 - 1)^2 + S_\mathrm{f}(I_3^{\mathrm{avg}} - 1)^2 \tag{5}$$

where I_3 is the third invariant (determinant) of the Right Cauchy–Green strain tensor and is a measure for the local volume for each Gaussian point. To conserve the local volumes (i.e., I_3 equals unity), the element is considered as incompressible solid. In contrast, if the weighted mean of all $I_3 s$ per element, (I_3^{avg}) is kept as unity, the element is considered to be a fluid. Using the penalty parameters S_s (for the solid volume) and S_f (for the fluid volume) (Table 1), the emphasis given for each part is determined.

2.1.2 Myofiber element

Maximally activated muscle is studied and within the muscle fibers, sarcomeres are assumed to have identical material properties. The force–velocity characteristics are not considered due to the isometric nature of the present work. The total stress for the intracellular domain ($\sigma_{22\mathrm{f}}$) is a Cauchy stress acting in the local fiber direction exclusively and is the sum of the active stress of the contractile elements ($\sigma_{22\mathrm{contr}}$) and the stress due to intracellular passive tension ($\sigma_{22\mathrm{icp}}$).

To define the active length-force characteristics, an exponential function (Fig. 1b) was fit to the experimental data of small rat gastrocnemius medialis (GM) fiber bundles (Zuurbier et al. 1995). This function is scaled such that at optimum length, the fiber direction strain (ε_{22}) is zero and the maximal stress value is unity.

$$\begin{aligned} &\sigma_{22\mathrm{contr}}(\varepsilon_{22}) = b_3 \mathrm{e}^{b_2\varepsilon_{22}^3} \quad \text{for } \varepsilon_{22} > 0 \text{ or} \\ &\sigma_{22\mathrm{contr}}(\varepsilon_{22}) = b_3 \mathrm{e}^{b_1\varepsilon_{22}^4} \quad \text{for } \varepsilon_{22} < 0 \\ &\text{where } b_1, b_2, \text{ and } b_3 \text{ are constants (Table 1)} \end{aligned} \tag{6}$$

The source of intracellular passive tension is the intrasarcomeric cytoskeleton (Trombitas et al. 1995), which is composed of several proteins. In this work titin is considered to play the dominant role. Experimental tension–sarcomere length data (Trombitas et al. 1995) for a single rabbit skeletal muscle fiber was fitted using a parabolic function (Fig. 1c) and scaled to make it compatible to the stress–strain characteristics of the contractile part.

$$\begin{aligned} &\sigma_{22\mathrm{icp}}(\varepsilon_{22}) = t_1\varepsilon_{22}^2 + t_2\varepsilon_{22} + t_3 \text{ and} \\ &\sigma_{22\mathrm{icp}}(\varepsilon_{22}) = 0 \text{ for } \varepsilon_{22} < 0 \\ &\text{where } t_1, t_2, \text{ and } t_3 \text{ are constants (Table 1)} \end{aligned} \tag{7}$$

Table 1 Values and definitions of the model constants

Constant	Value	Definition
k	0.05	Initial passive stiffness (Eq. 4)
a_{11}	8.0	Passive cross-fiber direction stiffness, $a_{11} = a_{33}$ (Eq. 4)
a_{22}	6.0	Passive fiber direction stiffness (Eq. 4)
a_{12}	6.0	Passive fiber–cross-fiber shear stiffness, $a_{12} = a_{23} = a_{31}$ (Eq. 4)
S_s	10.0	Weight factor in the penalty function for the solid volume (Eq. 5)
S_f	80.0	Weight factor in the penalty function for the fluid volume (Eq. 5)
b_1	30.0	Coefficient for the stress–strain relation of the contractile elements (Eq. 6)
b_2	–6.0	Coefficient for the stress–strain relation of the contractile elements (Eq. 6)
b_3	1	Coefficient for the stress–strain relation of the contractile elements (Eq. 6)
t_1	0.522	Coefficient for the stress–strain relation of the intracellular passive elements (Eq. 7)
t_2	0.019	Coefficient for the stress–strain relation of the intracellular passive elements (Eq. 7)
t_3	–0.002	Coefficient for the stress–strain relation of the intracellular passive elements (Eq. 7)

2.1.3 Elements linking fiber and matrix meshes

For the elastic links between the two meshes, which represent the transmembranous attachments of the cytoskeleton and ECM, a standard element COMBIN39, from the element library of ANSYS 9.0 was used. This is a two-node spring element, which is set to be uniaxial and have linear stiffness characteristics.

2.1.4 Aponeurosis element

To represent the aponeuroses, a standard 3D, eight-node element HYPER58, from the element library of ANSYS 9.0 is used. This element has a hyperelastic mechanical formulation for which the strain energy density function is defined using the Mooney–Rivlin material law.

It is assumed that, at the initial muscle length and in the passive state, the sarcomeres arranged in series within muscle fibers have identical lengths. Local strain, as a measure of change of length, reflects the lengthening (positive strain) or shortening (negative strain) of sarcomeres. Note that zero strain in the model represents the undeformed state of sarcomeres (i.e., sarcomere length $\cong 2.5\,\mu$m) in the passive condition at initial muscle length (28.7 mm). Fiber direction strain within the fiber mesh of the lfmm model was used to assess the nonuniformity of sarcomere lengths arranged in-series within muscle fibers (referred to as serial distribution). Muscle length equaling 25.2, 29.2, and 31.2 mm will be referred to as *low muscle length, intermediate muscle length,* and *high muscle length,* respectively.

2.2 Model of isolated intact extensor digitorium longus muscle

Extensor digitorium longus muscle of the rat was modeled. This muscle has a relatively simple geometry: it is a unipennate muscle with rather small pennation angles and minimal variation of the fiber direction within the muscle belly. The geometry of the model (Fig. 2a) is defined as the contour of a longitudinal slice at the middle of the isolated rat EDL muscle belly. Three muscle elements in series and six in parallel fill this slice. Therefore any collection of three muscle elements arranged in series represents a big muscle fascicle. All aponeurosis elements have identical mechanical properties but using a variable thickness in the fiber-cross fiber plane, the increasing cross-sectional area of the aponeurosis toward the tendon (Zuurbier et al. 1994) is accounted for.

2.3 Models of aponeurotomized extensor digitorium longus

In surgery, aponeurotomy is performed by cutting the muscles' aponeurosis transversely and passively lengthening the muscle. Experiments on aponeurotomized rat muscle showed that below the location of the intervention intramuscular connective tissue ruptures progressively in the muscle fiber direction after isometric activity at progressively higher muscle length (Jaspers et al. 1999). Presumably, such further rupturing occurs after the actual operation.

Therefore two types of interventions were modeled.

2.3.1 Model of aponeurotomized extensor digitorium longus with intact extracellular matrix

A separate application of the model was used to study the effects of aponeurosis discontinuity exclusively on muscle force and sarcomere length distributions: only the most proximal common nodes of two neighboring aponeurosis elements located in the middle of the proximal aponeurosis were disconnected. In such a model, despite the opening of small gap between the cut ends of the aponeurosis on muscle lengthening, no tear in the muscles' collagen fiber reinforced ECM is allowed. Therefore, it is possible to study the effects of this intervention per se, as the myofascial force transmission

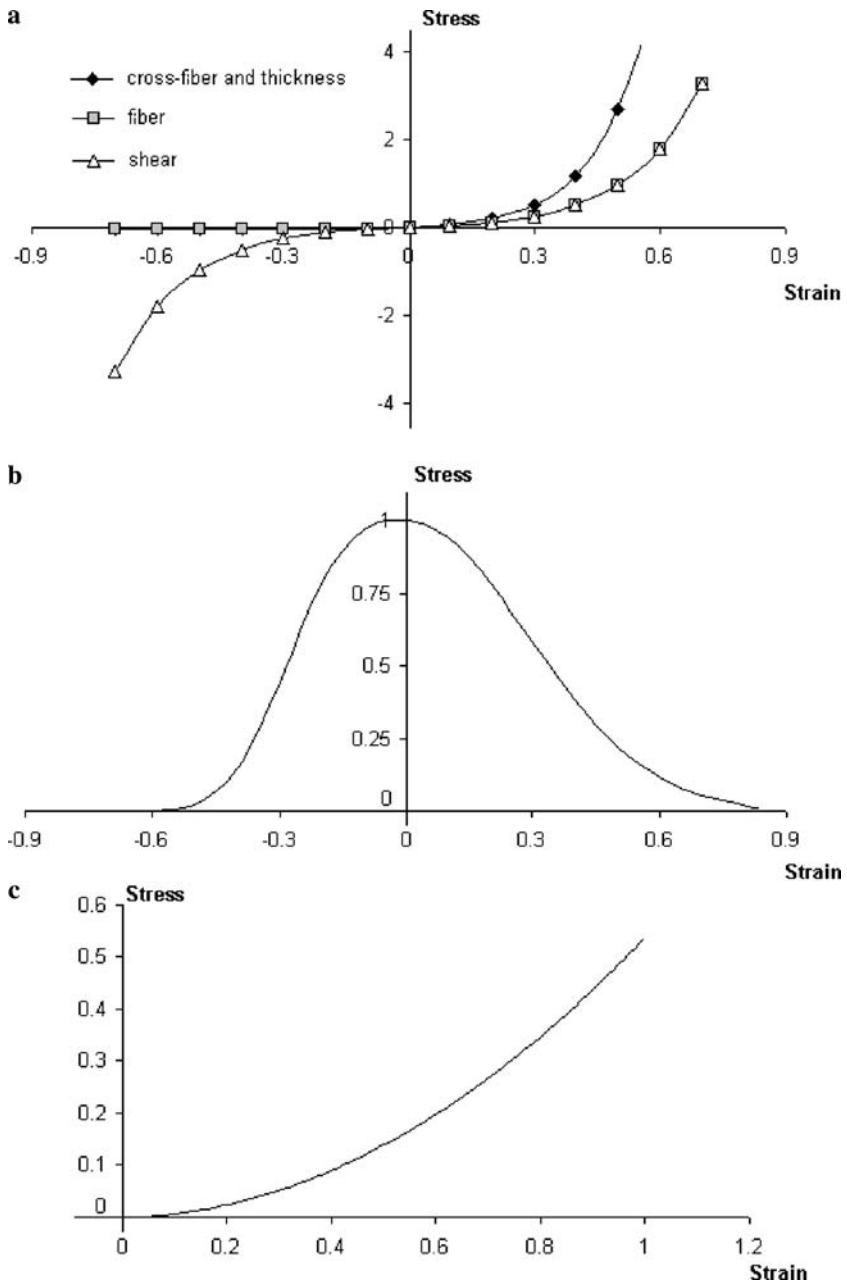

Fig. 1 The stress–strain characteristics of modeled muscle tissue. (**a**) Passive nonlinear and anisotropic material properties of the extracellular matrix element in the local coordinates. (**b**) Active stress–strain properties of the myofiber element representing the contractile apparatus, which is valid only for the local fiber direction. (**c**) Mechanical properties representing the titin filaments which is dominating the passive resistance in the myofiber element valid, also only in the local fiber direction. The curves in parts (**b**) and (**c**) are scaled to the maximum value of active contractile stress to make them compatible. The stresses are normalized and dimensionless

pathways are not interfered with. This model is referred to as *aponeurotomized EDL muscle with intact ECM*.

2.3.2 *Model of aponeurotomized extensor digitorium longus with torn extracellular matrix*

The full effects of proximal aponeurotomy were modeled by disconnecting the common nodes of two neighboring aponeurosis as well as muscle elements located in the middle of the proximal aponeurosis of the modeled muscle (Fig. 2a). As a consequence of the rupture, a wide gap opens between the cut ends of the aponeurosis. However, in the model the tear depth is limited by the length of these proximal muscle elements in the fiber direction. Figure 2b shows the typical deformed shape of the modeled *aponeurotomized EDL muscle* after distal lengthening and illustrates these features.

Presenting the results, the above models will be referred to as "intact", "aponeurotomized (intact ECM)" and "aponeurotomized", respectively.

2.4 Solution procedure

The analysis type used in ANSYS was static and large strain effects were included. During the entire solution procedure, the models studied were stable and no mesh refinement was performed. A force-based convergence criterion was used with a tolerance of 0.5%.

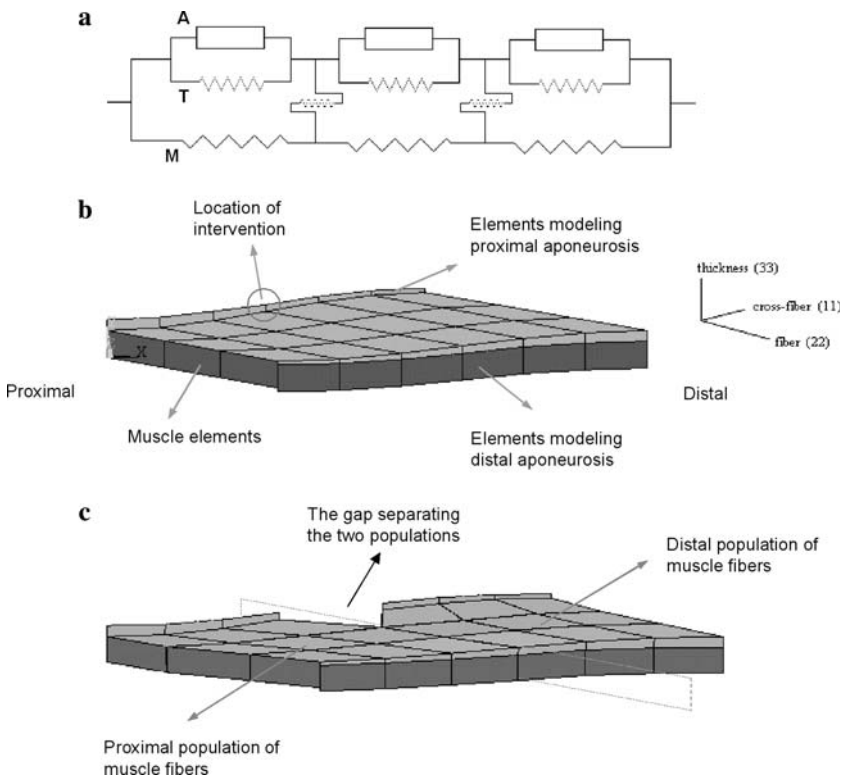

Fig. 2 Finite element modeling of isolated EDL muscle before and after aponeurotomy. (**a**) two-dimensional-schematic representation of an arrangement of muscle elements. The intracellular domain, which is composed of the active contractile elements (A) and intracellular passive cytoskeleton (T), is linked to the extracellular matrix domain (M) elastically. (**b**) The model of intact EDL muscle. The geometry of the finite element muscle model is defined by the contour of a longitudinal slice of the rat EDL muscle belly. The muscle model is composed of three muscle elements in series and six in parallel. A 3D local coordinate system representing the fiber, cross-fiber (normal to the fiber direction), and thickness directions is used for the analysis and presentation of the model results. Proximal aponeurotomy is modeled by disconnecting the common nodes of two neighboring aponeurosis elements located in the middle of the proximal aponeurosis of the modeled muscle. The disconnected nodes at the upper face of the model that are marked by a *circle* indicate the location of intervention modeled. Note that the nodes at the same location of the lower face of the model are also disconnected. (**c**) Typical example of the deformed shape of modeled proximally aponeurotomized muscle after distal lengthening. The modeled gap between the disconnected ends of the aponeurosis creates two distinct populations of muscle fibers that are referred to as "proximal population" and "distal population". The *plane marked by dotted lines* shows the interface between the two populations

Initially, at the passive state, the activation coefficient b_3 (Eq. 6) equaled 0. Maximal activation of the muscles modeled was achieved by increasing b_3 incrementally up to 1, using fixed increments. After activation, muscle length was changed by changing the position of muscle distal end: first in proximal direction (i.e., to shorten the muscle) then in distal direction (i.e., to lengthen the muscle). The position of muscle proximal end was fixed during the procedure. The total computation time was approximately 150 min.

3 Results

3.1 Effects of aponeurotomy on muscle length–force characteristics

For the fully isolated muscle, Fig. 3 shows muscle active and passive length–force characteristics for modeled intact EDL, aponeurotomized EDL muscle with intact ECM as well as aponeurotomized EDL muscle.

Near optimum length, differences between the length–active force characteristics of intact muscle and aponeurotomized EDL muscle with intact ECM are minor. After the intervention, muscle optimum length is unchanged, but a very small drop in muscle optimal force (only 1%) is found. In contrast, at lower lengths, the decrease in muscle active force is more pronounced (up to as much as 50%) (Fig. 3). Muscle active slack length shifted (by approximately 0.8 mm) to a higher length.

Passive forces of aponeurotomized EDL with intact ECM are higher than those of intact muscle. The absolute force difference increases with length. However, the normalized force difference decreases (becomes a smaller fraction of the passive force of intact muscle) as the muscle is lengthened: $\Delta F_{\text{passive}}$ for these two muscles is approximately 20% of the passive force of intact

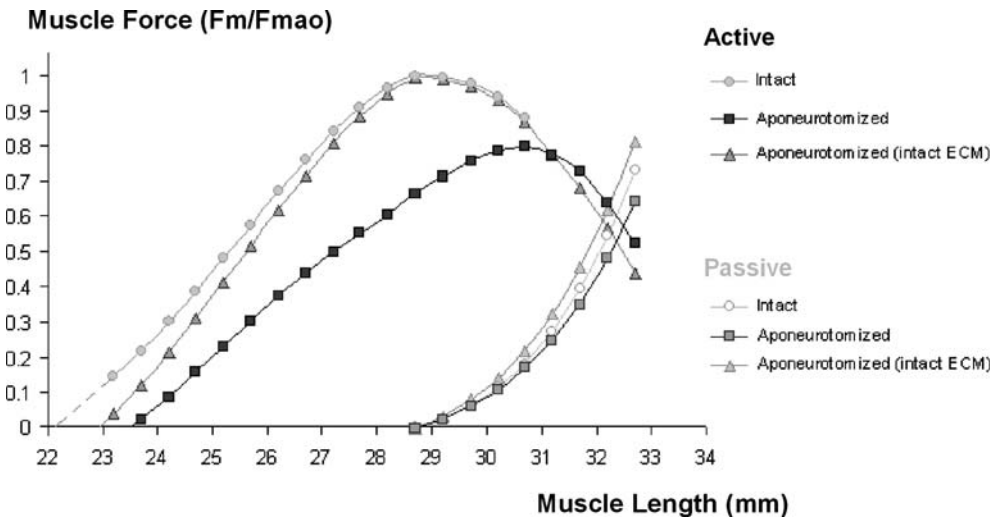

Fig. 3 The isometric muscle length–force characteristics of modeled EDL muscles. Active and passive isometric forces of intact muscle, aponeurotomized muscle and aponeurotomized muscle with intact extracellular matrix (ECM) are compared. All of data are normalized for optimal force of intact muscle

muscle at muscle length = 30.7 mm, whereas this fraction reduces to 11% at the highest length studied.

Length–active force characteristics of aponeurotomized EDL muscle differ substantially from both those of the intact muscle and of aponeurotomized EDL muscle with intact ECM. The optimum length of aponeurotomized muscle shifted to a higher muscle length (by 2.0 mm). Muscle active slack length of aponeurotomized muscle is shifted to a higher length (by approximately 1.2 mm with respect to intact muscle). Therefore, at any given length of the ascending limb of the length–force curve, muscle active force is lower. Muscle optimal force dropped to 79% of that of intact muscle.

Passive forces of aponeurotomized muscle are lower than those of intact muscle and the absolute and normalized force differences increase as the muscle is lengthened ($\Delta F_{\text{passive}}$ equals maximally 14% of the passive force of aponeurotomized muscle in the length range studied).

It is concluded that aponeurotomized muscle shows a sizable increase in the length range of active force exertion, as well as considerably lower active forces compared to intact muscle. This indicates major distributions of lengths of sarcomeres within muscle fibers such that the muscle contains also a substantial number of shortened sarcomeres (working on the descending limb of their length–force curve) even at high muscle lengths. However, if the muscles' ECM is left intact (i.e., if the myotendinous force transmission mechanism is partly interfered with exclusively) the effects of the intervention on muscle length–force characteristics are minor, but include an even somewhat decreased length range of force exertion.

3.2 Effects of surgical intervention with aponeurosis and intramuscular connective tissues

Figure 4a–c shows distributions of fiber direction strain as well as the deformed geometry of intact muscle at three different muscle lengths. Note that only a limited distribution of sarcomere lengths is found.

3.2.1 Effects of the discontinuity in the aponeurosis exclusively

Figure 4d–f shows distributions of fiber direction strain for aponeurotomized muscle with intact ECM at the three muscle lengths studied. A major result is that in general, both muscle geometry and fiber direction strain distributions show very minor differences compared to those of the intact muscle (Fig. 4a–f).

3.2.2 Effects of the discontinuities in the aponeurosis as well as the ECM on muscle geometry and distributions sarcomere length

Figure 5 shows distributions of fiber direction strain as well as the deformed geometry of aponeurotomized muscle at the same three muscle lengths. Characterized by tearing of intramuscular connective tissue, effects of aponeurotomy on geometry of muscle are substantial. Two cut ends of the aponeurosis are separated by a gap, the length of which increases as the muscle is lengthened. This creates two populations of muscle fibers: proximal population of muscle fibers (with intact myotendinous junctions at both ends) and distal population of muscle fibers (with no myotendinous connection to the muscles'

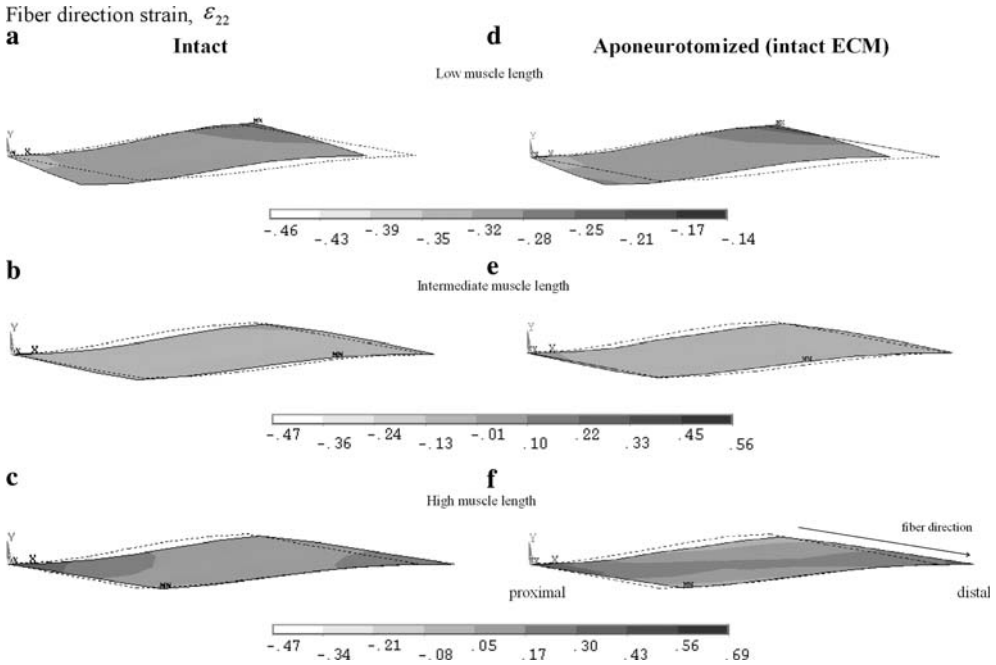

Fig. 4 Fiber direction strain within modeled intact muscle and within aponeurotomized muscle with intact extracellular matrix. *Left panel*: The strain distributions within the fiber mesh of active intact muscle. *Right panel*: The strain distributions within the fiber mesh of aponeurotomized muscle with intact extracellular matrix. The location of the intervention was at the middle of the proximal aponeurosis. Contour plots are shown for low muscle length (25.2 mm, i.e., (**a**) and (**d**)), intermediate muscle length (29.2 mm, i.e., (**b**) and (**e**)) and high muscle length (31.2 mm, i.e., (**e**) and (**f**)). The *dotted line contour* indicates passive muscle geometry at the initial length. The local fiber direction as well as the proximal and distal ends of the muscle are indicated (**f**)

origin). The proximal ends of muscle fibers in the distal population shift distally. This allows the muscle fibers to attain shorter lengths, which lead to increased fiber angles. For the proximal population, the constrained end of the proximal aponeurosis limits the position changes of the proximal ends of muscle fibers: no notable proximal shift occurs. However, the muscle fibers are lengthened and the fiber angle is decreased. We conclude that aponeurotomy and tearing of the muscle causes an increased distribution of fiber lengths within the muscle belly.

Such changes in the muscle geometry have major effects on lengths of sarcomeres within the aponeurotomized muscle. Accordingly, the sarcomeres at the proximal ends of the muscle fibers that are connected to either of the cut ends of the proximal aponeurosis are exposed to opposite and extreme length changes. For example at high muscle length, sarcomeres at the proximal edge of the cut aponeurosis are lengthened by 69%, whereas sarcomeres at the distal edge are shortened by 47% (Fig. 5c).

In contrast to the fairly homogeneous fiber direction strains shown for the intact muscle (Fig. 4a–c), the aponeurotomized muscle exhibits profound strain distributions (Fig. 5a–c) indicating major distributions of sarcomere lengths. Also note that the sarcomere length distributions in the distal population of muscle fibers and the proximal population of muscle fibers differ substantially. Therefore, effects of aponeurotomy on sarcomere length distributions are studied in further detail by distinguishing the two populations of muscle fibers within the aponeurotomized muscle.

Distal population of muscle fibers: A major model result is that the sarcomeres in the distal population of muscle fibers of the aponeurotomized muscle are substantially shorter than the sarcomeres within the muscle fibers of the intact muscle. For example, at low muscle length, the minimum shortening for the sarcomeres within the distal population of aponeurotomized muscle is approximately 32% (Fig. 5a) whereas this represents the value of maximum sarcomere shortening for the intact muscle (Fig. 4a). This effect becomes more dominant as the muscle is lengthened: at high muscle length all sarcomeres within the distal population of aponeurotomized muscle remain shortened by minimally 1% up to approximately 41% (Fig. 5c). In contrast, sarcomere lengthening of minimally 7% up to maximally 33% (Fig. 4c) is found for the intact muscle.

Note that the sarcomeres within those parts of distal population of muscle fibers near the tear have the shortest lengths and they show only minor length changes

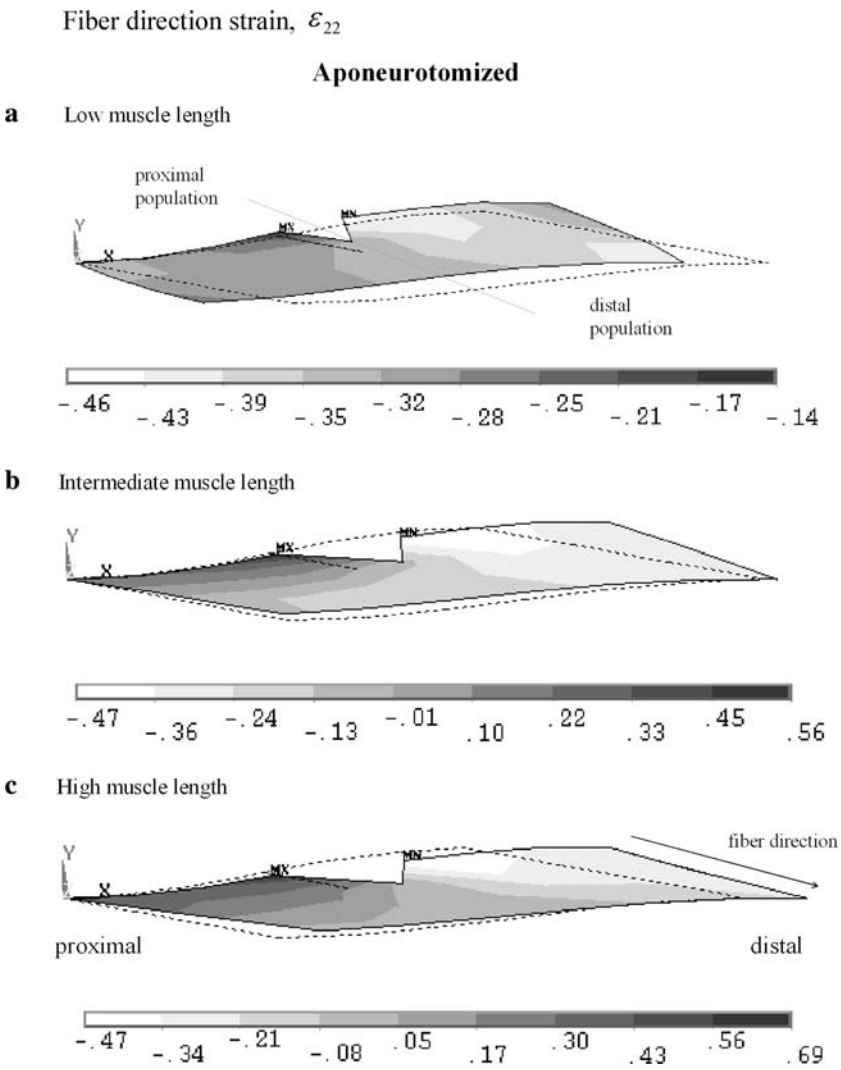

Fig. 5 Fiber direction strain within modeled aponeurotomized muscle. The strain distributions within the fiber mesh are shown as contour plots for (**a**) low muscle length (25.2 mm), (**b**) intermediate muscle length (29.2 mm), and (**c**) high muscle length (31.2 mm). The *dotted line contour* indicates passive muscle geometry at the initial length. Within each contour locations of maximal (MX) and minimal (MN) strain are marked. A *dotted line* (near MX) indicates the original position of the disconnected nodes in the passive muscle (i.e., no gap). The proximal and distal populations of muscle fibers in the aponeurotomized muscle are indicated by a line separating them (**a**). The local fiber direction as well as the proximal and distal ends of the muscle are indicated (**c**)

after muscle lengthening. However, lengthening of the muscle does alter the lengths of sarcomeres, which are located more distally within fibers of the distal population. For example, at low muscle length the sarcomeres located at the distal ends of muscle fibers are shortened by values ranging between 44 and 33% (Fig. 5a), whereas at high muscle length, such sarcomere shortening is still present but limited to values ranging between 22 and 3% (Fig. 5c). This shows the major role of intramuscular myofascial force transmission: the ECM connected to the muscle fibers via transsarcolemmal molecules prevents the sarcomeres within the muscle fibers of the distal population from shortening to their active slack length and also allows them to attain higher lengths with muscle lengthening.

Proximal population of muscle fibers: After the intervention, sarcomeres within the proximal population of muscle fibers are not as short. However, as a result of myofascial force transmission, aponeurotomy does affect substantially the distribution of lengths of sarcomeres also for the proximal population. In contrast to the homogeneity in sarcomere lengths shown for the intact muscle (Fig. 4a–c), the aponeurotomized muscle shows a major serial distribution of lengths of sarcomeres within this population of fibers (Fig. 5a–c). This distribution becomes more pronounced as the muscle is lengthened distally: the sarcomeres at the proximal ends of muscle fibers are lengthened substantially whereas the ones located distally are much shorter. For example at high muscle length, the most proximally located sarcomeres are lengthened by 43–69% whereas the more distal sarcomeres remain shortened up to approximately 21% (Fig. 5c).

We conclude that the added discontinuity in the ECM affect lengths of sarcomeres in a major way such that sarcomere length distributions show contrasting effects for the two populations of muscle fibers after proximal aponeurotomy: (1) In the distal population, generally

the lengths of sarcomeres are much shorter than the lengths of sarcomeres in the proximal population. (2) From proximal ends of muscle fibers to distal ends, sarcomere lengths in the distal population vary from the lowest length to higher lengths. (3) However, such variation is reversed in the proximal population and it includes sarcomeres at very high lengths at the proximal ends of muscle fibers.

An important conclusion is that the acute effects of the intervention are determined primarily by the discontinuity in the ECM, rather than the discontinuity in the aponeurosis exclusively.

Reflecting the effects of sarcomere length distributions, stress in the fiber mesh shows the contribution of sarcomeres at different locations to active muscle force. The fiber direction stresses in the intact muscle do not show a notable distribution (Fig. 6a,–c). For aponeurotomized muscle with intact ECM, stress distributions (Fig. 6d–f) show very minor differences compared to those of the intact muscle.

In contrast, for the aponeurotomized muscle stress distribution is substantial (Fig. 7a–c).

Distal population of muscle fibers: The stress values calculated for the sarcomeres of the distal population of the aponeurotomized muscle are substantially lower than the values calculated for the intact muscle. For example, at intermediate muscle length, stress in the intact muscle is homogeneous at values equaling unity (Fig. 6b), whereas stress in the distal population of the aponeurotomized muscle varies between values from approximately zero to maximally 0.38 (Fig. 7b). This shows that the reduced muscle active force found acutely after the intervention is ascribable largely to the dominance of short sarcomeres in the distal population of muscle fibers.

However, stress distributions in the distal population of muscle fibers also show that the majority of the sarcomeres contribute to the muscle force at all muscle lengths despite lacking myotendinous connections to the muscles' origin. This is true even for the shortest of the sarcomeres within the distal population (i.e., the sarcomeres located at the proximal ends of muscle fibers, near the tear). At low muscle length, a sizable number of sarcomeres near the tear show very low stress values, maximally 0.11 (Fig. 7a). However, even these sarcomeres do not attain their active slack length. As the muscle is lengthened, the number of sarcomeres with such low stress decreases substantially. At high muscle length, only the sarcomeres located at the proximal ends of the muscle fibers near the tear show values ranging between 0.01 and 0.13 (Fig. 7c). In contrast, the sarcomeres, which are located more distally within fibers of the distal population, show much higher stress values, up to 0.72. This shows that including the ones located near the tear, myofascial force transmission prevents sarcomeres from shortening to nonphysiological lengths allowing almost all of them to contribute to muscle force.

Proximal population of muscle fibers: Figure 7 shows that although the differences in stress distributions are not as substantial as for the distal population, stress values calculated for the proximal population are also lower than the values calculated for the intact muscle. For example, at intermediate muscle length, compared to the stress value equal to approximately unity in the intact muscle (Fig. 6b), the stress in the proximal population of the aponeurotomized muscle is lower than that (minimally 0.6) for a sizable part of the muscle fibers (Fig. 7b).

We conclude that the reduced active muscle force acutely after aponeurotomy is primarily due to the short sarcomeres in the distal population. However, the highly lengthened proximal sarcomeres in the proximal population of muscle fibers also contribute to the reduction of active force.

For the aponeurosis elements of the muscles modeled in the passive state, Fig. 8 shows the strain distributions in the global x-direction (i.e., in the direction of the muscle line of pull). The aponeuroses of the passive intact muscle are strained more than those of the aponeurotomized muscle (Fig. 8a, b). On the other hand, the aponeuroses of the passive aponeurotomized muscle with intact ECM show more straining than those of the intact muscle (Fig. 8b, c). Note that these differences correlate with the corresponding passive force differences shown in Fig. 3.

4 Discussion

Aponeurotomy is a surgical intervention performed to improve the impeded function for patients with neurological disorders. Therefore, it is important to understand the mechanisms of this intervention in order to consider possibilities for enhancing the effects of the operation. In this study, mechanical aspects of this mechanism were investigated: (1) muscle length–force characteristics and (2) sarcomere length distributions within the muscle fibers were studied.

4.1 Intended effects of aponeurotomy on muscle length–force characteristics in relation to myotendinous and myofascial force transmission mechanisms

In, for example, cerebral palsy, hypertonia is a common symptom that causes the muscle affected to remain

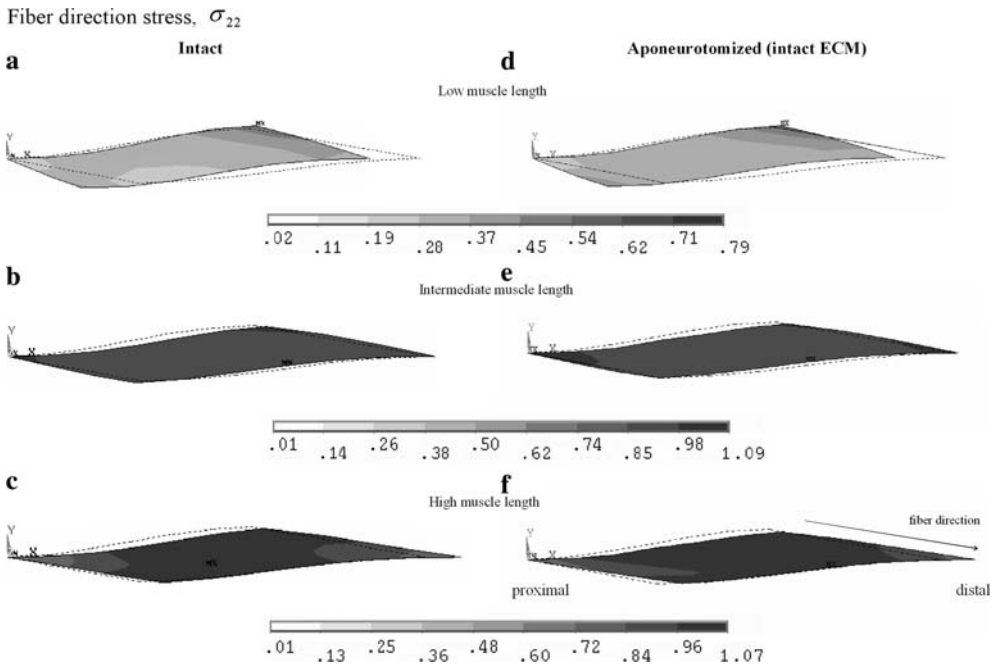

Fig. 6 Fiber direction stress within modeled intact muscle and within aponeurotomized muscle with intact extracellular matrix. *Left panel*: The stress distributions within the fiber mesh of intact muscle. *Right panel*: The stress distributions within the fiber mesh of aponeurotomized muscle with intact extracellular matrix. Contour plots are shown for low muscle length (25.2 mm, i.e., (**a**) and (**d**)), intermediate muscle length (29.2 mm, i.e., (**b**) and (**e**)) and high muscle length (31.2 mm, i.e., (**e**) and (**f**)). The *dotted line contour* indicates muscle geometry at the initial length. The local fiber direction as well as the proximal and distal ends of the muscle are indicated (**f**)

at rather low length. Adaptation to such a sustained state causes muscle contractures and the overly short muscle restricts joint motion. Therefore, a major goal of aponeurotomy is to lengthen the muscle and to restore a more normal joint range of motion.

Our present model results show that acutely after aponeurotomy leading to a discontinuity in the muscles' ECM, both muscle active slack length and muscle optimum length shift to higher muscle lengths and the length range of force exertion increases as the shift in optimum length is greater. These features agree well with earlier experimental results obtained acutely after aponeurotomy. For rat GM muscle (Jaspers et al. 1999) and for EDL muscle (Jaspers et al. 2002) similar shifts in active slack length and optimum length of the aponeurotomized muscle were reported such that the length range of force exertion increased. However, if the discontinuity is limited to the aponeurosis exclusively (a condition not attainable experimentally), our present results showed no shift in muscle optimum length. Moreover, a shift in muscle active slack length to a higher muscle length was found showing that the muscle length range of force exertion is actually decreased.

On the other hand, unusual positions of a joint and contractures may result also from imbalance of antagonistic muscles. Weakening of the agonist muscle (i.e., reducing muscle force) may increase the relative effect of the antagonistic muscles. Aponeurotomy has been indicated as a clinical means of such weakening (e.g. Nather et al. 1984).

Our present results show after aponeurotomy and ECM discontinuity a substantial reduction of muscle active force for all muscle lengths. However, if the muscles' ECM is not discontinuous such reduction was almost negligible at intermediate and higher muscle lengths and is much more limited at low muscle lengths. This shows that although half of the muscle fibers lack myotendinous connections via the proximal aponeurosis to the muscles' origin, almost all of the force produced within these fibers is transmitted to the proximal tendon via the fully intact intramuscular myofascial pathways for force transmission. A similar effect of a discontinuity in the intramuscular connective tissues on reduction of muscle force was shown in intramuscular fasciotomy experiments after tenotomy in the multiheaded rat EDL muscle. In contrast to a minor decrease in muscle force

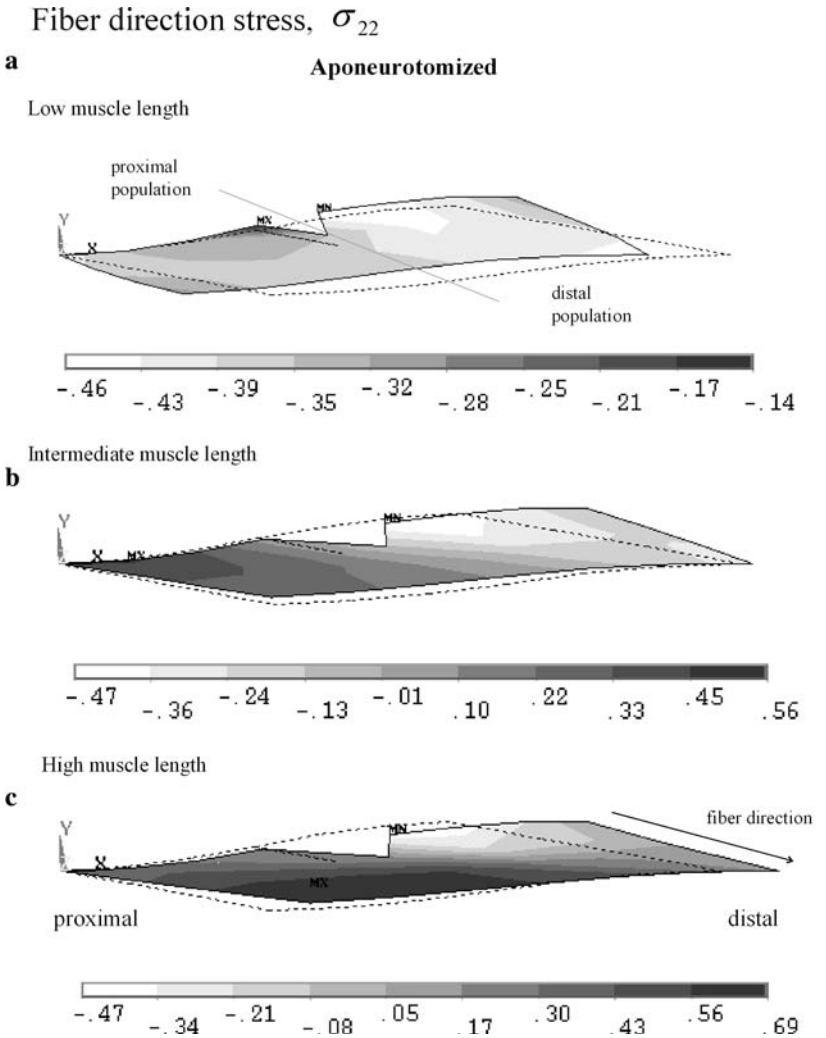

Fig. 7 Distributions of fiber direction stress within modeled aponeurotomized muscle. The stress distributions within the fiber mesh are shown as contour plots for (**a**) low muscle length (25.2 mm), (**b**) intermediate muscle length (29.2 mm), and **c** high muscle length (31.2 mm). The *dotted line contour* indicates passive muscle geometry at the initial length. Within each contour locations of maximal (MX) and minimal (MN) stress are marked. A *dotted line* (near MX) indicates the original position of the disconnected nodes in the passive muscle (i.e., no gap). The proximal and distal populations of muscle fibers in the aponeurotomized muscle are indicated by a line separating them (**a**). The local fiber direction as well as the proximal and distal ends of the muscle are indicated (**c**)

found after exclusively cutting the distal tendons of selected heads, dissecting the fascial interface between the two most distal EDL heads (Huijing et al. 1998) resulted in a major reduction of force (e.g., optimum force was reduced by 50%).

We conclude that the desired effects of surgical aponeurotomy in terms of both increased muscle tendon complex length at a given joint angle, as well as increased length range of force exertion and reduction in muscle force are almost entirely a result of the interference with myofascial force transmission pathways. This indicates that major attention should be given to definition and manipulation of length and activity of the muscle also after the operation, as this will affect the acute effects of the surgical intervention. Immediately after surgery, the limb is usually placed in a cast. The length of the muscle within the cast is expected to be a major determinant. If deeper tears within the muscle are judged necessary a higher length of casting would be indicated. The degree of isometric activity of the aponeurotomized muscle within the cast may also enhance the acute effect of surgery by causing deeper tears of the intramuscular connective tissues.

4.2 Sarcomere length distributions as the key determinant of the effects on muscle length–force characteristics

Our present results indicate that a discontinuity in the aponeurosis exclusively does not alter considerably the sarcomere length distributions compared to the intact muscle. This is because in both cases, the intramuscular connective tissues are fully intact and the interaction of the muscular stroma with the muscle fibers constrains sarcomere length changes. However, in the case of connective tissue tears (ECM discontinuity), especially affecting the part of the muscle belly distal to the location of the intervention and determined by the depth of the tear, the capability of restraining sarcomere shortening in contracting muscle is reduced

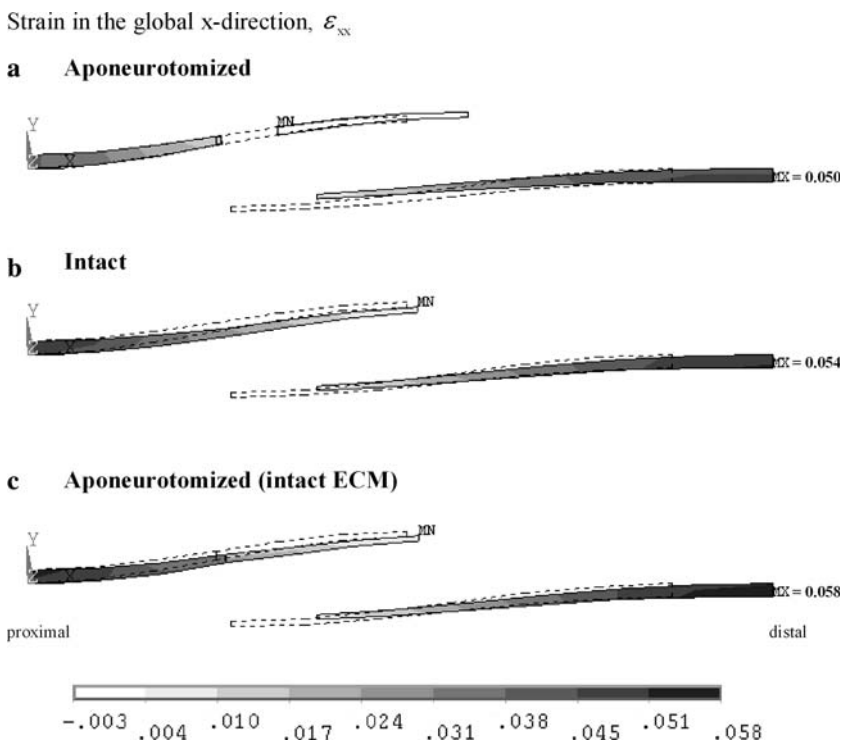

Fig. 8 Distributions of strain within the aponeuroses for the muscles in passive state. Distributions within the aponeurosis elements are shown for the global *x*-direction (i.e., in the direction of the muscle line of pull). (**a**) Aponeurotomized muscle. For this condition the gap between the cut ends aponeurosis of the proximal aponeurosis is clearly visible. (**b**) Intact muscle. (**c**) Aponeurotomized muscle with intact extracellular matrix. Muscle length equals 32.7 mm. The *dotted line contour* indicates geometry of the aponeuroses at the initial length. Note that the position of the distal aponeurosis is changed due to muscle lengthening and associated muscle fiber length and angle changes. Locations of maximal values of strain calculated for the distal ends of the distal aponeuroses are indicated (MX). The proximal and distal ends of the muscle are indicated (only in (**c**)). X in the proximal end of the proximal aponeurosis indicates the global *x*-direction

substantially. This explains the highly shortened sarcomeres in the distal population. On the other hand, because a sizable part of the muscle lengthening is taken up by the proximal ends of muscle fibers of the proximal population located between the proximal tendon and the cut end of the aponeurosis, most proximal sarcomeres attain higher lengths than the ones located distally within the same muscle fibers. We conclude that the intervention leads to an altered myofascial force transmission, which yields a complex distribution of lengths of sarcomeres.

Such distribution has major effects on muscle length–force characteristics. For the aponeurotomized muscle, the shift in muscle optimum length to higher lengths is explained by the substantial inhomogeneity of sarcomere lengths. In earlier experiments on intact muscle, serial sarcomere length distribution (Wohlfart et al. 1977; Morgan et al. 2000) and heterogeneity of mean sarcomere length of different fibers (Willems and Huijing 1994; Huijing 1998) were shown to enhance the muscle length range of force exertion.

On the other hand, differences in sarcomere lengths at low muscle lengths affect muscle active slack length. This length is determined by the last sarcomere that manages to overcome opposing internal forces within the fiber and muscle and exert force on the outside world. Therefore, for a shift in active slack length to higher lengths to occur, as shown presently for aponeurotomized muscles, the following has to be the case: The last sarcomeres reaching very low lengths, but just capable of exerting force externally has to reach this state at a higher muscle length. Additional modeling shows that at very low muscle lengths (results not presented), the sarcomeres within the aponeurotomized muscle are generally shorter than those in the aponeurotomized muscle with intact ECM, which in turn are shorter than those in the intact muscle. Therefore, as the aponeurotomized muscle is at active slack length (all sarcomeres are too short to exert force externally), the intact muscle still contains sarcomeres that are at higher lengths allowing a higher active force. Therefore, the shifts in muscle active slack length to higher lengths shown for

aponeurotomized muscle with or without intact ECM are explained by the altered distributions of sarcomere lengths due to the intervention.

Similar to experimental results of Jaspers et al. (1999), Brunner et al. (2000) also showed experimentally a shift in muscle optimum length and active slack length to higher lengths for rat GM muscle acutely after aponeurotomy. However, these authors found a greater shift for muscle active slack length than for optimum length. Therefore, despite the lengthening effect, muscle length range of force exertion was narrowed. In the light of our findings, differences in sarcomere length distributions within the GM muscle among the two studies are conceivable. A likely cause for this can be the differences in depth of tear within the intramuscular connective tissues. Our present modeling showed that the absence of a discontinuity in the ECM leads to a narrowed length range of force exertion.

At the ascending limb of length–force characteristics, the lower muscle active forces are ascribable primarily to the dominance of short sarcomeres within the distal fiber population and partially also to the highly lengthened proximal sarcomeres within the proximal fiber population. Note that the shift in muscle active slack length also contributes to the lower muscle active forces at higher lengths on the ascending limb of the length–force curve. The decrease in muscle optimum force due to aponeurotomy in our present results was 21%. An experimental decrease of 29% in muscle optimum force was reported by Jaspers et al. (2002) for EDL.

We conclude that the complex distribution of lengths of sarcomeres determines the effect of the intervention.

4.3 Passive force

Regarding the comparison of intact and aponeurotomized muscles, our results show that the intervention leads to a decrease in muscle passive force and the force difference increases as the muscle length increases. This is in agreement with experimental results (Jaspers et al. 1999). Our modeling allows an analysis of the mechanical reasons for the force decrease. The aponeuroses of the intact passive muscle are strained more in the direction of the muscles' line of pull than those of the aponeurotomized muscle. Two main effects associated with the major changes of muscle geometry after the intervention are responsible for that effect and the lower muscle passive forces: (1) Shear strains between the cross-fiber and fiber directions within the aponeurotomized muscle are substantially different from those of the intact muscle. Note also the contrasting effects for the two populations of muscle fibers within the aponeurotomized muscle. For a large part of the proximal population, higher shear strain is found, leading to a more pronounced decrease in muscle fiber angle than in the intact muscle. In contrast, in the distal population, the fiber angle is higher for the aponeurotomized muscle because the shear strain works in the opposite direction. Such effects of shear in the aponeurotomized muscle lead to a translational position change for the part of the proximal aponeurosis distal to the location of intervention and for the proximal end of the distal aponeurosis. This allows limited straining of aponeurotic tissues. (2) Lengths of muscle fibers of the proximal population are similar to those in the intact muscle. However, muscle fibers of the distal population are considerably shorter than their counterparts in the intact muscle. Note that even negative fiber direction strain is found at the distal ends of a sizable number of muscle fibers. Such negatively strained parts in the passive aponeurotomized muscle yield very low (close to zero) stress. Also the lower strain values found elsewhere within this fiber population are notable. These two factors reduce the stress in the matrix mesh, which is an important explanation of the lower passive force.

Note also that the negative fiber direction strains within the distal population of the passive aponeurotomized muscle are illustrative for the major role of intramuscular myofascial force transmission in intact muscle and the interference with such transmission determining the acute effects of the intervention, because the altered geometry of the ECM allows the passive sarcomeres to attain shorter lengths.

On the other hand, our present results showed higher passive forces for aponeurotomized muscle with intact ECM compared to intact muscle. As this condition is not possible to produce experimentally, no experimental data is available for a comparison. However, modeling of this condition shows how important the tearing of the ECM is for the effect of the surgery: The muscle geometry is very similar before and after the intervention as long as the ECM is not torn. Therefore, the strain distributions show only minor differences with those of the intact muscle. Only the fiber direction strains lead to small but consistent differences between the muscle fibers for the two conditions, such that all fibers of the intact muscle are longer. This explains the lower aponeurosis strain found for the intact muscle as a relatively larger fraction of the effects of muscle lengthening is taken up by the muscle fibers rather than by the aponeuroses. Therefore, the aponeurotic tissues being stiffer than the ECM allows a higher muscle passive force to be exerted by the aponeurotomized muscle with intact ECM. However, this effect decreases at higher muscle lengths and so does the normalized passive force difference between the two conditions.

4.4 Limitations of FEM modeling on acute effects of aponeurotomy

Our present study investigates the effects of a discontinuity in the muscle tissue due to aponeurotomy. However, the progressive nature of the rupturing (Jaspers et al. 1999, 2002; Brunner et al. 2000) was not represented: at all muscle lengths studied, the model involves a certain tear depth as determined by the length of the most proximal muscle elements in the fiber direction. Nevertheless, Jaspers et al. (1999, 2002) showed that after increasing the muscle length immediately after the intervention, subsequent repetitive determination of muscle active isometric forces yielded no further rupture (i.e., the tear depth was stabilized) and reproducible measurements. Therefore, our present modeling represents the muscle with a stabilized tear depth.

However, the tear observed in the experimented muscles was deeper: for example for proximally aponeurotomized rat EDL it was up to about half of the fiber length (Jaspers et al. 2002). It is expected that a deeper tear causes a further reduction of active muscle force and further increase in the length range of force exertion. Results of an earlier 2D finite element modeling study of proximal aponeurotomy of rat GM muscle (Rekveldt 1999) with different tear depths (25, 50, and 75% of the fiber length) support this. Nevertheless, our present model shows the principles of the mechanical mechanism of the intervention. Note that although the depth of tear is an important determinant of the favorable acute effects of aponeurotomy, it is not easy to control this in practice.

The mechanical properties of EDL muscle modeled presently represent the properties of healthy muscle. Intramuscular connective tissues are comprised of complex structures of collagen, stiffness of which tissues depends on the collagen content of the muscle as well as on the morphology. Collagen content in spastic muscle of children with cerebral palsy was shown to correlate positively with the severity of the disorder (e.g. Booth et al. 2001). This suggests that spastic muscles are stiffer than healthy muscles. At the whole muscle level there is experimental data supporting this (e.g. Tardieu et al. 1982; Sinkjaer and Magnussen 1994). At the cellular level, Friden and Lieber (2003) showed that the elastic modulus of the muscle fibers taken from patients with spasticity is greater than that of healthy muscle fibers. It is conceivable that a stiffer ECM than presently modeled can provide more resistance to sarcomere shortening, which may lead to a less pronounced effect in the distal population of muscle fibers. However, the basic principles of the mechanical mechanism of the intervention would remain the same.

It should be noted that for long-term effects, the mechanical properties of muscle tissue are subject to complex adaptive mechanisms, effects of which needs to be studied in future studies.

The multimolecular structures (Berthier and Blaineau 1997) that connect muscle fibers to the ECM consist of several proteins. In our model this complex system is lumped into linear elastic intramuscular linking elements. Although no specific data are available on their mechanical properties, it is conceivable that these connections have nonlinear mechanical properties. Therefore, their stiffness may be variable and possibly be more compliant at lower strains. This may affect the sarcomere length distributions within the aponeurotomized muscle. For an explorative testing of this effect, we used tri-linearly stiff elements in both of our aponeurotomized muscle models such that the linking stiffness was minimally 50, 67, or 100% of the value used in the calculation of our results presented. In addition, the 100% value was reached at a 50% higher strain. Such variable compliance linking caused only minor changes in fiber direction strain distributions of aponeurotomized muscle within our models (results not shown). For example the zone of maximal strains may be somewhat narrower, but the general pattern of distribution was quite similar. Therefore, we expect such effects to be small. However, new studies designed to determine the mechanical properties of these multimolecular structures are necessary and this may allow an improved representation within our model.

On the other hand, in our model, the mechanical properties of the intramuscular linking elements are selected to ensure a physiological condition. If very compliant links are used, we showed earlier local strain concentrations within the muscle (e.g. extreme sarcomere lengthening which are interpreted as so-called "popped sarcomeres") and nonphysiological length–force characteristics, representing pathological conditions (Yucesoy et al. 2002). This may represent the deficiency of dystrophin or other molecules of the chain connecting the muscle fiber to the ECM that lead to muscular dystrophies (e.g. Campbell 1995; Jung et al. 1996; Ohlendieck 1996). As the mechanical properties of the intramuscular linking elements used presently avoid such pathological effects, our present results reflect specific effects of aponeurotomy.

4.5 Further implications of the present results

Positive contributions of aponeurotomy to decreasing the degree of muscle spasticity were reported earlier (e.g. Suso et al. 1985; Reimers 1990). In spastic conditions, limiting the lengthening of muscle fibers will lead

to limited receptor activity of the muscle spindles. The dominance of short sarcomeres found presently for the distal population of muscle fibers even at higher lengths indicates reduced strain on the muscle spindles. Such length depended effects are also expected for the velocity dependent stretch effects of muscle spindles that are dynamically sensitive. Such limited sarcomere lengthening is an acute effect of aponeurotomy and is expected to cause some reduction of the degree of spasticity for a sizable part of the muscle belly. However, for the proximal fiber population, sarcomeres towards the proximal ends of muscle fibers are lengthened considerably at higher muscle lengths. This probably indicates a limit to reducing the effects of spasticity. These results suggest that, manipulating the role of myofascial force transmission, the location of the intervention may be optimized to achieve favorable surgical results.

Due to intramuscular myofascial force transmission, our present results indicate contribution of nearly all of the sarcomeres to muscle force even acutely after aponeurotomy. If during recovery from the operation, the continuity of the muscles' aponeurosis and ECM is reestablished (Brunner et al. 2000; Jaspers et al. 2005) both paths of myofascial force transmission and myotendinous force transmission will be reconstructed. Therefore, the acute effects of aponeurotomy and progressive tearing of muscle which leads to short sarcomeres that produce very low force are expected to be removed in the long term and the weakening effect is not likely to fully persist. Complete recovery of muscle force was reported by Brunner et al. (2000). In recent morphological and histological studies, new connective tissue was reported to reconnect the cut ends of the 10–15% longer aponeurosis after recovery (Jaspers et al. 2005). This new tissue is more compliant than the regular aponeurotic tissue. It is conceivable that a lengthened and more compliant aponeurosis can sustain the effects of aponeurotomy also in the long term (e.g., Brunner et al. 2000). However, despite the remaining muscle lengthening, these authors showed for rat GM a decreased muscle length range of force exertion after recovery. In the light of our present results, the mechanism of such limiting of length range could be a reduced distribution of sarcomere lengths, explained by the remodeled myofascial force transmission pathways, after the reestablishment of the integrity of the ECM within the tear.

In conclusion, our present study shows that a complex mechanism of sarcomere length distribution is central to the determination of the desired effects of aponeurotomy on muscle length–force characteristics to correct functional abnormalities. Manipulation of such distributions depends on interfering with myofascial force transmission pathways, which determines the acute effects of the intervention, rather than interfering with the myotendinous force transmission mechanism after which the operation was named. This indicates that conditions of muscle tendon complex length and degree of isometric activity also during the casted phase after the operation require major attention. Taking into account effects of intramuscular myofascial force transmission will help setting optimal goals and optimizing success of the surgical operation.

Acknowledgments This work was supported by (1) the Vrije Universiteit, Amsterdam, (2) the Universiteit Twente, Enschede, and (3) Boğaziçi University Research Fund under grant BAP04HX102 to Can A. Yucesoy.

References

Baumann JU, Koch HG (1989) Ventrale aponeurotische Verlangerung des Musculus Gastrocnemius. Oper Orthop Traumatol 1:254–258

Berthier C, Blaineau S (1997) Supramolecular organization of the subsarcolemmal cytoskeleton of adult skeletal muscle fibers. A review. Biol Cell 89:413–434

Booth CM, Cortina-Borja MJ, Theologis, TN (2001) Collagen accumulation in muscles of children with cerebral palsy and correlation with severity of spasticity. Dev Med Child Neurol 43:314–320

Brunner R, Jaspers RT, Pel JJ, Huijing PA (2000) Acute and long-term effects on muscle force after intramuscular aponeurotic lengthening. Clin Orthop Relat Res 378:264–273

Campbell KP (1995) Three muscular dystrophies: loss of cytoskeleton–extracellular matrix linkage. Cell 80:675–679

Ejeskar A (1982) Finger flexion force and hand grip strength after tendon repair. J Hand Surg 7:61–65

Friden J, Lieber RL (2003) Spastic muscle cells are shorter and stiffer than normal cells. Muscle Nerve 27:157–164

Gielen S (1998) A continuum approach to the mechanics of contracting skeletal muscle. PhD thesis Eindhoven University of Technology, Eindhoven, The Netherlands

Hawkins D, Bey M (1997) Muscle and tendon force–length properties and their interactions in vivo. J Biomech 30:63–70

Hijikata T, Wakisaka H, Niida S (1993) Functional combination of tapering profiles and overlapping arrangements in nonspanning skeletal muscle fibers terminating intrafascicularly. Anat Rec 236:602–610

Huijing PA (1998) Muscle the motor of movement: properties in function, experiment and modeling. J Electromyogr Kinesiol 8:61–77

Huijing PA (1999a) Muscle as a collagen fiber reinforced composite material: force transmission in muscle and whole limbs. J Biomech 32:329–345

Huijing PA (1999b) Muscular force transmission: a unified, dual or multiple sytem? A review and some explorative experimental results. Arch Physiol Biochem 170:292–311

Huijing PA, Baan GC, Rebel G (1998) Non myo-tendinous force transmission in rat extensor digitorum longus muscle. J Exp Biol 201:682–691

Huyghe JM, van Campen DH, Arts T, Heethaar RM (1991) The constitutive behaviour of passive heart muscle tissue: a quasi-linear viscoelastic formulation. J Biomech 24:841–849

Jaspers RT, Brunner R, Pel JJM, Huijing PA (1999) Acute effects of intramuscular aponeurotomy on rat GM Force transmission, muscle force and sarcomere length. J Biomech 32:71–79

Jaspers RT, Brunner R, Baan GC, Huijing PA (2002) Acute effects of intramuscular aponeurotomy and tenotomy on multitendoned rat EDL: indications for local adaptation of intramuscular connective tissue. Anat Rec 266:123–135

Jaspers RT, Brunner R, Riede UN, Huijing PA (2005) Healing of the aponeurosis during recovery from aponeurotomy: morphological and histological adaptation and related changes in mechanical properties. J Orthop Res 23:266–273

Johansson T, Meier P, Blickhan R (2000) A finite-element model for the mechanical analysis of skeletal muscles. J Theor Biol 206:131–149

Jung D, Duclos F, Apostol B, Straub V, Lee JC, Allamand V, Venzke DP, Sunada Y, Moomaw CR, Leveille CJ, Slaughter CA, Crawford TO, McPherson JD, Campbell KP (1996) Characterization of delta-sarcoglycan, a novel component of the oligomeric sarcoglycan complex involved in limb-girdle muscular dystrophy. J Biol Chem 271:32321–32329

Lieber RL, Friden J (1997) Intraoperative measurement and biomechanical modeling of the flexor carpi ulnaris-to-extensor carpi radialis longus tendon transfer. J Biomech. Eng 119:386–391

Morgan DL, Whitehead NP, Wise AK, Gregory JE, Proske U (2000) Tension changes in the cat soleus muscle following slow stretch or shortening of the contracting muscle. J of Physiol 522(Pt 3):503–513

Nather A, Fulford GE, Stewart K (1984) Treatment of valgus hindfoot in cerebral palsy by peroneus brevis lengthening. Dev Med Child Neurol 26:335–340

Nene AV, Evans GA, Patrick JH (1993) Simultaneous multiple operations for spastic diplegia. Outcome and functional assessment of walking in 18 patients. J Bone Joint Surg 75B:488–494

Ohlendieck K (1996) Towards an understanding of the dystrophin–glycoprotein complex: linkage between the extracellular matrix and the membrane cytoskeleton in muscle fibers. Eur J Cell Biol 69:1–10

Olney BW, Williams PF, Menelaus MB (1988) Treatment of spastic equinus by aponeurosis lengthening. J Pediatr Orthop 8:422–425

Oomens CW, Maenhout M, van Oijen CH, Drost MR, Baaijens FP (2003) Finite element modelling of contracting skeletal muscle. Philos Trans Roy Soc Lond Ser B Biol Sci 358:1453–1460

Ramsey RW, Street SF (1940) The isometric length-tension diagram of isolated skeletal muscle fibers of the frog. J Cell Comp Physiol 15:11–34

Reimers J (1990) Functional changes in the antagonists after lengthening the agonists in cerebral palsy. I. Triceps surae lengthening. Clin Orthop Relat Res 253:30–34

Rekveldt MGC (1999) Finite element modeling of aponeurotomy. M.Sc. thesis, in Faculty of Mechanical Engineering, University of Twente, Enschede, The Netherlands

Sinkjaer T, Magnussen I (1994) Passive, intrinsic and reflex-mediated stiffness in the ankle extensors of hemiparetic patients. Brain 117:355–363

Street SF (1983) Lateral transmission of tension in frog myofibers: a myofibrillar network and transverse cytoskeletal connections are possible transmitters. J Cell Physiol 114:346–364

Street SF, Ramsey RW (1965) Sarcolemma: transmitter of active tension in frog skeletal muscle. Science 149:1379–1380

Suso S, Vicente P, Angles F (1985) Surgical treatment of the nonfunctional spastic hand. J Hand Surg 10:54–56

Tardieu C, Huet de la Tour E, Bret MD, Tardieu G (1982) Muscle hypoextensibility in children with cerebral palsy: I. Clinical and experimental observations. Arch Phys Med Rehabil 63:97–102

Trombitas K, Jin JP, Granzier H (1995) The mechanically active domain of titin in cardiac muscle. Circ Res 77:856–861

Trotter JA, Purslow PP (1992) Functional morphology of the endomysium in series fibered muscles. J Morphol 212:109–122

Trotter JA, Richmond FJ, Purslow PP (1995) Functional morphology and motor control of series-fibered muscles. Exerc Sport Sci Rev 23:167–213

van der Linden BJJJ (1998) Mechanical modeling of muscle functioning. PhD thesis, Faculty of Mechanical Engineering, University of Twente, Enschede, The Netherlands

Willems ME, Huijing PA (1994) Heterogeneity of mean sarcomere length in different fibres: effects on length range of active force production in rat muscle. Eur J Appl Physiol Occup Physiol 68:489–496

Wohlfart B, Grimm AF, Edman KA (1977) Relationship between sarcomere length and active force in rabbit papillary muscle. Acta Physiol Scand 101:155–164

Yucesoy CA, Koopman HJFM, Huijing PA, Grootenboer HJ (2002) Three-dimensional finite element modeling of skeletal muscle using a two-domain approach: linked fiber–matrix mesh model. J Biomech 35:1253–1262

Zuurbier CJ, Everard AJ, van der Wees P, Huijing PA (1994) Length–force characteristics of the aponeurosis in the passive and active muscle condition and in the isolated condition. J Biomech 27:445–453

Zuurbier CJ, Heslinga JW, Lee-de Groot MB, Van der Laarse WJ (1995) Mean sarcomere length–force relationship of rat muscle fibre bundles. J Biomech 28:83–87